CHAPTER 65

A NUMERICAL MODEL OF THE ROUGH TURBULENT BOUNDARY LAYER IN COMBINED WAVE AND CURRENT INTERACTION

HUYNH-THANH Son and TEMPERVILLE André
Institut de Mécanique de Grenoble
B.P. 53X, 38041 Grenoble Cedex, France

ABSTRACT

The turbulent boundary-layer flow over flat rough beds due to a wave or a combined wave-current interaction is studied by using a simplified numerical second-order turbulence model. The model results are compared with many sets of experimental data. Excellent predictions for ensemble-averaged velocities and favourable predictions for turbulence quantities are obtained. Variations of kinematic and dynamic characteristics of boundary-layer flow with wave, current and bed roughness parameters are determined. The model is also modified to simulate the oscillatory turbulent flow over rippled beds. The mean velocity field and the distribution of time-averaged turbulence quantities are calculated. The validity of the model is verified through comparison with experimental results. The performance and the limitation of the model are discussed.

I. INTRODUCTION

A knowledge of the boundary layer flow in the vicinity of the sea bed is important for problems of coastal engineering, in particular for investigations of coastal erosion, sediment transport and the transport of pollutants.

Bodies of water that are subjected to currents and waves, according to their characteristics, produce a flat, generally rough bed, or a rippled bed. In order to quantify sediment transport, the amplitude and direction of the velocities and shear stresses in the boundary layer close to these different shapes of bed must be known.

Enquiries into the turbulent boundary layer generated by a sinusoidal wave are not recent. The experiments of Jonsson (1963), Horikawa and Watanabe (1968), Kamphuis (1975), Jonsson and Carlsen (1976) are noteworthy. Recently, experiments have been performed using laser velocimetry, e.g. the experiments of

Sumer et al. (1986), Sleath (1987) and Jensen et al. (1989). Theoretically, numerous investigations exist : from the analytical models of Kajiura (1968), Brevik (1981), Myrhaug (1982), Trowbridge and Madsen (1984) to the numerical models of Bakker (1974), Johns (1975), Sheng (1984), Fredsoe (1984), Asano and Iwagaki (1986), Blondeaux (1986), Justesen (1988), Sheng and Villaret (1989). Also to be mentioned is the semi-empirical model of Jonsson (1980), which proposed a universal distribution law for the velocity in the boundary layer.

As far as the boundary layer due to the interaction between a current and a wave is concerned, few experiments are available, among which only those of Van Doorn (1979), Simon et al. (1988) pertain to the turbulent and hydraulically rough case that is of interest to us. After the analytical model of mixing length due to Bijker (1967), other analytical models are based on the time-invariant turbulent viscosity, as in the case of a wave : Lundgren (1973), Smith (1977), Grant and Madsen (1979), Tanaka and Shuto (1984), Myrhaug (1984), Asano and Iwagaki (1984). For numerical models, that of the mixing length due to Bakker and Van Doorn (1978), Van Kerstern and Bakker (1984) as well as that of Fredsoe (1984), which assumes a logarithmic velocity distribution. Models with more or less complicated turbulent closure are also applied to this problem : Sheng (1984), and Davies et al. (1988).

To investigate the effect of wave and current on the boundary layer, we have selected the second order turbulence model that was originally suggested by Lewellen (1977) and simplified by Sheng (1984), Sheng and Villaret (1989) for the one dimensional flows. A simplified three dimensional version of the model is actually developed for the case of a wave without and with current. The numerical results are compared with experimental results in order to verify the validity of the model. In the last section, the model is written in orthogonal curvilinear coordinates in order to investigate oscillatory turbulent flow over a rippled bed. The results obtained are also compared with the experimental results for the case of symmetric and asymmetric ripples.

II. BOUNDARY LAYER ABOVE A FLAT BED

II-1. *Equations of the model*

The problem is treated in cartesian coordinates (x,y,z) with the z axis directed upwards (Fig. 1). The flat horizontal bottom is fixed at $z = z_0 = k_N/30$, where k_N represents the equivalent Nikuradse roughness.

The system of equations is established with the following assumptions: (*a*) the thickness of the boundary layer is much smaller than the wavelength of the wave; (*b*) the amplitude of the wave velocity $\hat{U}_h$ is much smaller than the wave celerity C.

In these conditions, the momentum equations for the two horizontal components of velocity (u,v) along x and y can be written:

$$(1) \quad \frac{\partial u}{\partial t} = -\frac{1}{\rho}\frac{\partial P}{\partial x} + \frac{\partial}{\partial z}(-\overline{u'w'}) \quad ; \quad (2) \quad \frac{\partial v}{\partial t} = -\frac{1}{\rho}\frac{\partial P}{\partial y} + \frac{\partial}{\partial z}(-\overline{v'w'})$$

where the Reynolds stresses $-\overline{u'w'}$ and $-\overline{v'w'}$ can be modelled in the form :

$$(3) \qquad -\overline{u'w'} = \nu_t \frac{\partial u}{\partial z} \quad , \quad -\overline{v'w'} = \nu_t \frac{\partial v}{\partial z}$$

where ν_t represents the turbulent viscosity.

The pressure gradients are expressed as follows :

$$(4) \qquad -\frac{1}{\rho}\frac{\partial P}{\partial x} = \frac{\partial U_{hx}}{\partial t} - \frac{1}{\rho}\frac{\partial P_c}{\partial x} \quad , \quad -\frac{1}{\rho}\frac{\partial P}{\partial y} = \frac{\partial U_{hy}}{\partial t} - \frac{1}{\rho}\frac{\partial P_c}{\partial y}$$

where (U_{hx}, U_{hy}) are the two horizontal components of the wave velocity and P_c represents the pressure due to the current.

Turbulent closure is performed by means of two equations for the turbulent kinetic energy K and for the length scale L of the turbulence (Lewellen, 1977) :

$$(5) \qquad \frac{\partial K}{\partial t} = \nu_t \left[\left(\frac{\partial u}{\partial z}\right)^2 + \left(\frac{\partial v}{\partial z}\right)^2 \right] - \frac{\nu_t}{L^2} K + 1.2 \frac{\partial}{\partial z}\left(\nu_t \frac{\partial K}{\partial z}\right)$$

$$(6) \qquad \frac{\partial L}{\partial t} = 0.175 \frac{\nu_t}{K} \left[\left(\frac{\partial u}{\partial z}\right)^2 + \left(\frac{\partial v}{\partial z}\right)^2 \right] L + 0.075 \sqrt{2}\, K + 1.2 \frac{\partial}{\partial z}\left(\nu_t \frac{\partial L}{\partial z}\right) - \frac{0.375\sqrt{2}}{\sqrt{K}} \cdot \left[\frac{\partial (\sqrt{K}\, L)}{\partial z} \right]^2$$

The assumption of local equilibrium of the turbulence made by Sheng (1984) allows ν_t to be put in the form :

$$(7) \qquad \nu_t = \sqrt{2} \frac{\sqrt{K}\, L}{4}$$

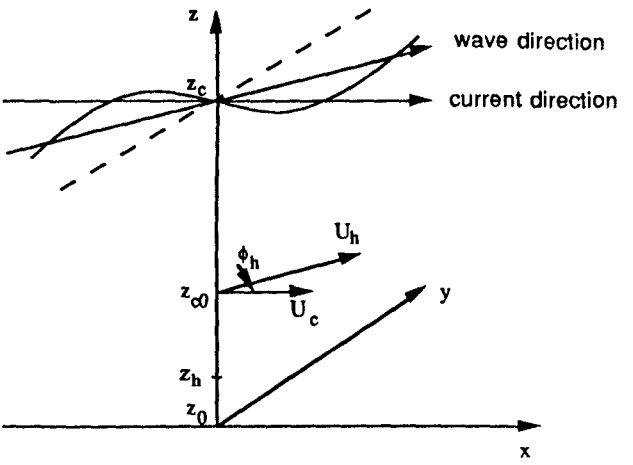

Fig. 1 *Outline of physical system and reference system of axes (flat bed)*

At the bottom ($z = z_0$) the boundary conditions in all cases are the following :

(8) $u = v = 0 \quad ; \quad \partial K/\partial z = 0 \quad ; \quad L = \alpha z_0 \quad$ with $\alpha = 0.67$,

where the von Karman constant is taken as $k = 0.4$.

The conditions at the upper limit of the boundary layer depend on the particular case studied, and will be described later.

The set of equations (1) to (8) is discretised using the implicit finite control volume method (Patankar, 1980) on a grid whose step size increases exponentially from bottom to top, thus giving good resolution near the bed where gradients are important. The time step is constant over the whole period of the wave. Each discretised equation corresponds to a tridiagonal matrix which can be solved by means of Thomas's algorithm (Roache, 1976).

II-2. *Case of the wave*

In the case of a unidirectional wave, the above set of equations is solved by taking $v = 0$. The pressure gradient is given by :

(9) $$-\frac{1}{\rho}\frac{\partial P}{\partial x} = \frac{\partial U_h}{\partial t}$$

where $U_h = \hat{U}_h \sin \omega t$ is the wave velocity at the upper limit of the boundary layer defined by $z_h = \delta_K$, δ_K corresponds to the thickness beyond which K is zero. The following approximation was obtained :

(10) $$\frac{\delta_K}{k_N} = 0.246 \left[\frac{\hat{a}_h}{k_N} \right]^{0.81} \quad \text{with} \quad \hat{a}_h = \frac{\hat{U}_h}{\omega}$$

For $z = z_h$ the boundary conditions are :

(11) $$K = L = 0 \text{ and } U = U_h$$

* *Comparison with experimental results* : The model results were compared with the experiment of Sumer et al. (1986). The lower boundary is at $z_0 = k_N/30 = 0.0133$ cm, and the upper boundary is taken to be at $z_h = 20$ cm. The magnitude of the wave velocity is $\hat{U}_h = 210$ cm/s and the period $T = 2\pi/\omega = 8.1$ s. Good agreement can be seen in Figure 2 for the velocities, except at $z = 0.1$ cm. The values of the friction velocity $u_* = \text{sign}(-\overline{u'w'}) \sqrt{|-\overline{u'w'}|}$ are slightly lower than found experimentally (Fig. 3). In Figure 4 the profiles of the fluctuating velocities $\sqrt{\overline{u'^2}}$ and $\sqrt{\overline{w'^2}}$ are compared. It can be seen that there is agreement for $\sqrt{\overline{u'^2}}$ for phases between 30° and 120°, and for $\sqrt{\overline{w'^2}}$ for the other phases.

* *Wave friction coefficient* : In investigations of the wave boundary layer, the friction coefficient f_h introduced by Jonsson (1963) is often used : $\frac{\hat{\tau}}{\rho} = \frac{1}{2} f_h \hat{U}_h^2$

where $\hat{\tau}$ is the amplitude of the shear stress at the bed. The formula for f_h that arises

from the present model as follows :

$$f_h = 0.00278 \exp\left[4.65 \left(\frac{\hat{a}_h}{k_N}\right)^{-0.22}\right] \tag{12}$$

For comparison, Figure 5 shows the curves obtained from the formulae of Kajiura (1968), Kamphuis (1975), Jonsson and Carsen (1976). The curve given by (12) is close to the results of Kamphuis.

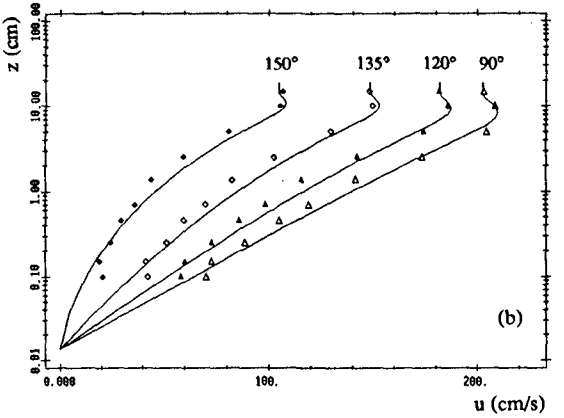

Fig. 2 Comparison between the calculated velocity profiles (——) and those measured by Sumer et al (1986) (symbols) for the different phases.

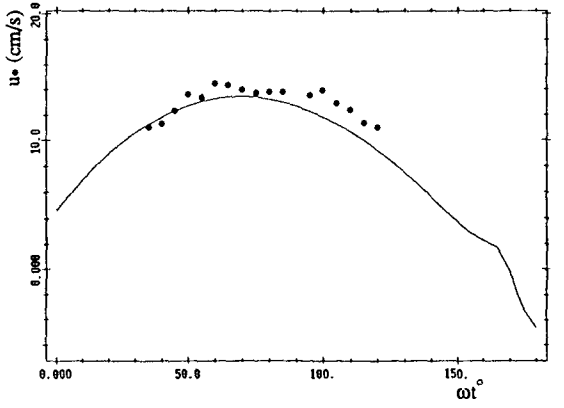

Fig. 3 Comparison between the shear velocity calculated by the present model (——) and that obtained experimentally by Sumer et al (1986) (●)

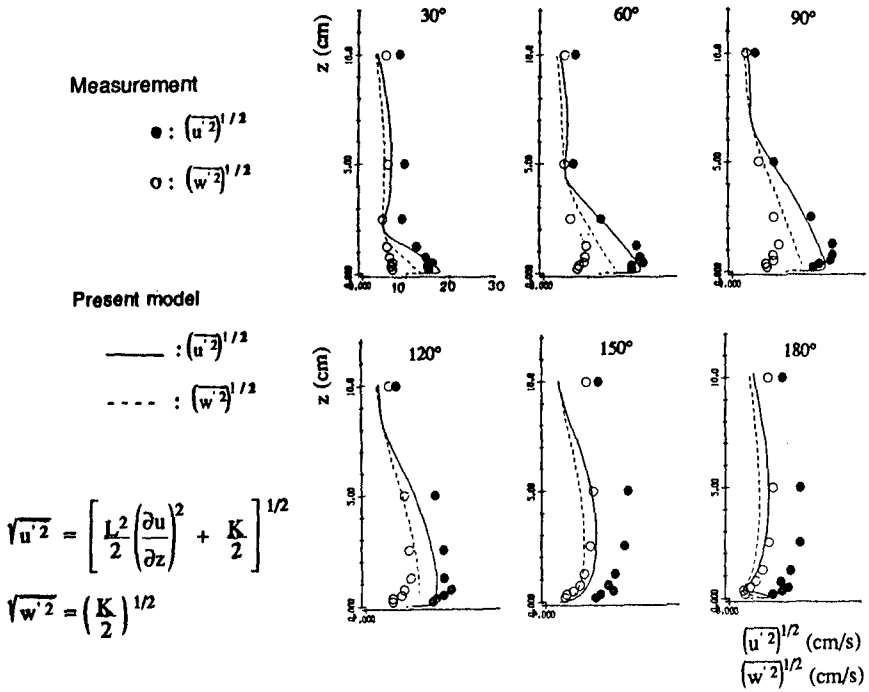

Fig. 4 Comparison between the fluctuating velocity profiles calculated by the present model and and those obtained experimentally by Sumer et al. (1986) for the different phases.

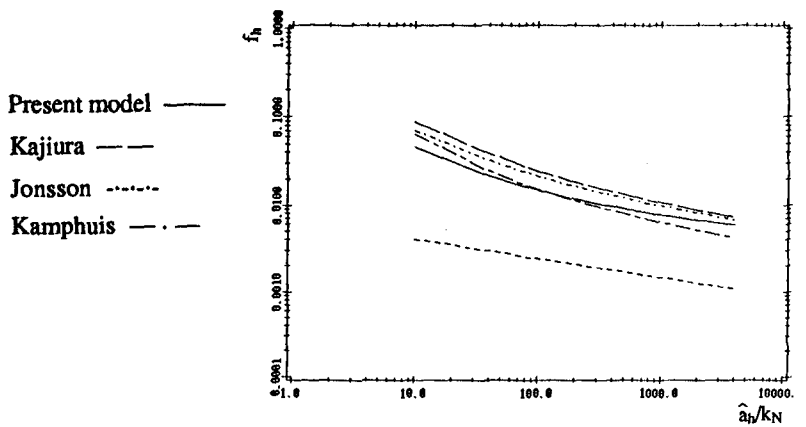

Fig. 5 Variation of the friction coefficient f_h as a function of $\hat{a}_h/k_N$

II-3. *Case of wave and current interaction*

The investigation of the wave-current interaction is performed using equations (1)+(8). The wave propagates in a direction at an angle ϕ_h to the current, which is parallel to the direction x (Fig. 1). The upper boundary conditions apply at $z = z_{c0}$ located in the inertial layer of the current and which is taken to be at (0.10+0.15) z_c, where z_c is the total height. The two components of the velocity at z_{c0} are assumed to be known :

(13) $\quad U = U_c + U_{hx} = U_c + U_h \cos \phi_h \quad ; \quad V = U_{hy} = U_h \sin \phi_h$

where U_c is the current velocity.

In addition, the following boundary conditions are applied:

(14) $\quad u = U \; ; \; v = V \; ; \; \partial K/\partial z = 0 \; ; \; L = \alpha z \; ; \; \partial P_c/\partial x = \partial P_c/\partial y = 0$

* *Comparison with experimental results* : The results of the model are compared with the experiments of Van Doorn (1981) for the case of colinear wave-current interaction ($\phi_h = 0°$). We selected the test V20RA, for which the upper limit z_{c0} is equal to 4.5 cm. In Figure 6 is shown the mean velocity profile. Good agreement is found with the experiment. The upper limit can be also treated at the surface libre z_c = 30 cm (Huynh Thanh and Temperville, 1989).

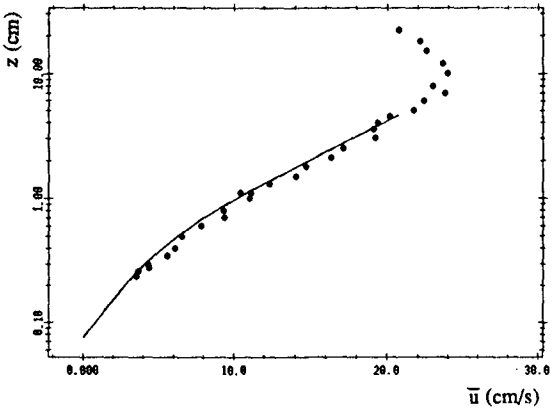

Fig. 6 Comparison between the mean velocity profiles calculated with the present model (——) and those measured by Van Doorn (1981). Test V20RA.

* *Friction coefficients* : The friction coefficients f_{ch} and f_c are defined as follows :

(15) $$\frac{\hat{\tau}_{ch}}{\rho} = \frac{1}{2} f_{ch} \hat{U}_h^2 \quad ; \quad \frac{\bar{\tau}_c}{\rho} = \frac{1}{2} f_c \hat{U}_h^2$$

where $\hat{\tau}_{ch}/\rho$ and $\bar{\tau}_c/\rho$ are the maximum and mean shear stresses respectively.

Figures 7 and 8 show the variation of f_{ch} and f_c as a function of $\hat{a}_h/k_N$ for different values of z_{c0}/k_N, $U_c/\hat{U}_h$, and ϕ_h. From these curves, it can be noted that for fixed z_{c0}/k_N and ϕ_h, f_{ch} and f_c increase for increasing $U_c/\hat{U}_h$. The change in f_c with ϕ_h is substantial only for $U_c/\hat{U}_h < 1$. When the current is stronger than the wave ($U_c/\hat{U}_h \geq 1.5$+2), the influence of ϕ_h on f_c is not marked, which means that in this case the mean characteristics of the current practically do not change under the action of the wave.

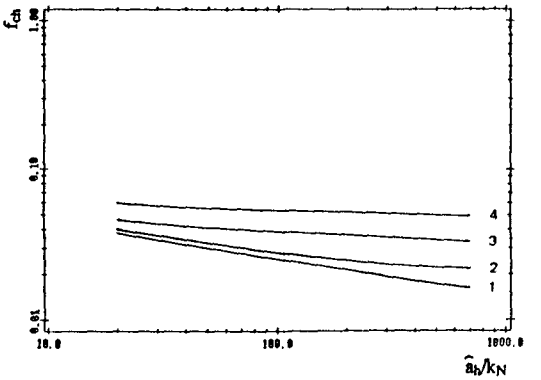

Fig. 7 . Variation of the friction coefficient f_{ch} as a function of $\hat{a}_h/k_N$, z_{c0}/k_N, $U_c/\hat{U}_h$ and ϕ_h. $z_{c0}/k_N = 100$ $\phi_h = 0°$

(1) $U_c/\hat{U}_h = 0{,}5$ (2) $U_c/\hat{U}_h = 1$ (3) $U_c/\hat{U}_h = 1{,}5$ (4) $U_c/\hat{U}_h = 2$

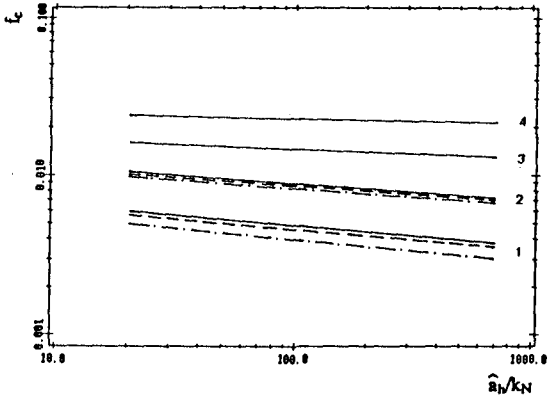

Fig. 8 Variation of the friction coefficient f_c as a function of $\hat{a}_h/k_N$, z_{c0}/k_N, $U_c/\hat{U}_h$ and ϕ_h. Parameters and notations as in Fig.7.

—— $\phi_h = 0°$; – – – $\phi_h = 45°$; – · – · – $\phi_h = 90°$

III. BOUNDARY LAYER ON A RIPPLED BED

III-1. *Formulation of the model*

The physical problem is outlined in Figure 9 : under the action of a wave of wavelength L_h, maximum velocity $\hat{U}_h$ and period T, two-dimensional vortex ripples are assumed to be present on the bed. Laboratory and *in situ* measurements have shown that $L_h >> L_r$. This allows us to restrict the zone of the calculation : rather than investigating the problem over the whole of the wavelength L_h, we shall only consider the wavelength L_r as shown in Figure 9. Moreover, to simplify the description of the boundary conditions at the surface of the ripple and also to eliminate the unknown pressure gradient due to the bed form, it is convenient in this case to transform the cartesian coordinates (x,z) into orthogonal curvilinear coordinates (X,Z), and to use the variables ψ (stream function) and ξ (vorticity) instead of the velocities u and w.

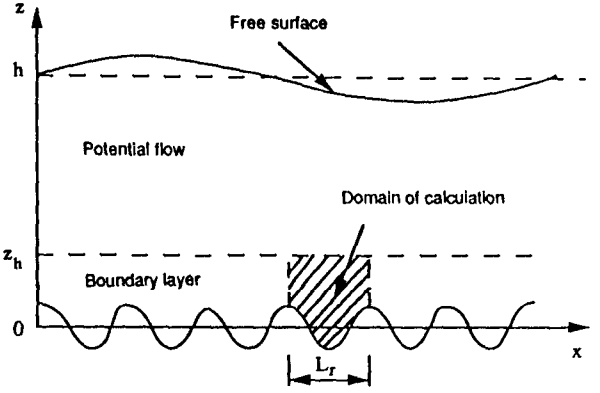

Fig. 9 Scheme of the physical system (rippled bed).

In general, the coordinate transformation is given by :

$$X = x + \sum_{n=1}^{N} a_n . \exp(-n k_r Z) . \sin(n k_r X - \theta_n) \tag{16}$$

$$Z = z - \sum_{n=1}^{N} a_n . \exp(-n k_r Z) . \cos(n k_r X - \theta_n)$$

where a_n and θ_n are the amplitude and phase difference of the nth harmonic describing the ripple, and $k_r = 2\pi/L_r$ is the wave number associated with L_r.

The stream function ψ and the vorticity ξ are defined by :

$$u = \frac{\partial \psi}{\partial z} \quad ; \quad w = -\frac{\partial \psi}{\partial x} \quad ; \quad \xi = \frac{\partial u}{\partial z} - \frac{\partial w}{\partial x} \tag{17}$$

In coordinates (X,Z), the set of equations to be solved is :

(18) $$J \nabla^2 \psi = \xi$$

(19) $$\frac{1}{J}.\frac{\partial \xi}{\partial t} - \frac{\partial (\psi, \xi)}{\partial (X, Z)} = \nabla^2 (\nu_t \xi) - J \zeta$$

(20) $$\frac{1}{J}.\frac{\partial K}{\partial t} - \frac{\partial (\psi, K)}{\partial (X, Z)} = 1{,}2 \frac{\partial}{\partial X}\left(\nu_t \frac{\partial K}{\partial X}\right) + 1{,}2 \frac{\partial}{\partial Z}\left(\nu_t \frac{\partial K}{\partial Z}\right) + \nu_t J \left[\left(\frac{\partial^2 \psi}{\partial X^2}\right)^2 + \left(\frac{\partial^2 \psi}{\partial Z^2}\right)^2\right] - \frac{1}{J}.\nu_t K - \frac{1}{J}.\frac{\nu_t}{L^2} K$$

The length scale L is assumed to vary as follows :

(21) $$L = \alpha Z \sqrt{1 - \frac{Z}{Z_h}}$$

and the turbulent viscosity ν_t is determined by (7).

In the previous set of equations, ζ and **K** are terms pertaining to the partial derivatives of ψ and ν_t; J is the jacobian of the coordinate transformation ; ∇^2 is the laplacian operator. The following boundary conditions are applied :

- At the lower limit of the boundary layer ($Z = Z_0 = k_N/30$)

(22) $$\frac{\partial \psi}{\partial Z} = \frac{\partial \psi}{\partial X} = \psi = \frac{\partial K}{\partial Z} = 0 \quad ; \quad \xi_0 = \frac{2 J \psi_1}{(Z_1 - Z_0)^2}$$

where ψ_1 is the stream function at height Z_1 on the second node of the grid (Roache, 1976).

- At the upper limit of the boundary layer ($Z = Z_h$)

(23) $$\psi = Z_h U_h (t) \quad ; \quad K = \xi = 0$$

- At the lateral boundaries ($X = 0$ and $X = L_r$), we assume spatially periodic conditions for ψ, ξ and K.

The above set of equations is discretized using implicit finite difference schemes (centred in space and forward in time). The alternating direction implicit (A. D. I.) method is used to solve the equations for ξ and K. The Poisson equation for ψ is solved by the bloc-cyclic reduction method (Roache, 1976) which allows a huge saving in calculation time compared with the Gauss-Seidel iteration method. The spatial grid contains MxN nodes with step ΔX = const, and ΔZ varying exponentially from the bottom upwards. The time step is $\Delta t = T/360$ s. In all the test cases, convergence is obtained after 20 calculation periods.

III-2. *Comparison with the experimental results of Du Toit and Sleath (1981)*

The dimensional parameters in the test for comparison are the following :

- Symmetric ripple with $L_r = 17.2$ cm, $h_r = 2.9$ cm, $d = 0.04$ cm

- Cosinusoidal wave : $U_h = \hat{U}_h \cos \omega t$, where $\hat{U}_h = 14.3$ cm/s, $T = 2\pi/\omega = 5.37$s

For the numerical calculation, a 17x25 node grid was chosen with $\Delta X = 1.0625$ cm and ΔZ varying from 0.056 cm to 0.5 cm. The equivalent Nikuradse roughness is $k_N = 2.5\ d = 0.1$ cm. The upper limit is chosen to be equal to $Z_h = 5$ cm.

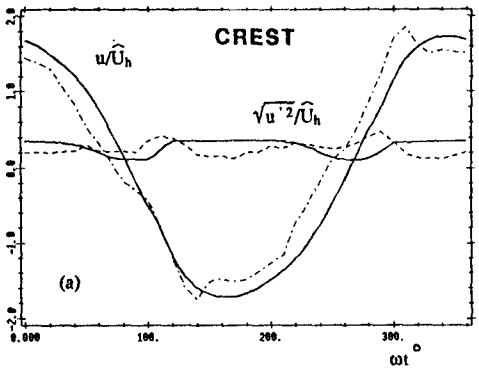

Fig. 10 Comparison between the results of present model (——) and those of the measurements of Du Toit and Sleath (1981) for the time variation of the horizontal velocity u and of the horizontal fluctuating velocity $\sqrt{u'^2}$.
Measurements at height z = 1.65 cm above the crest

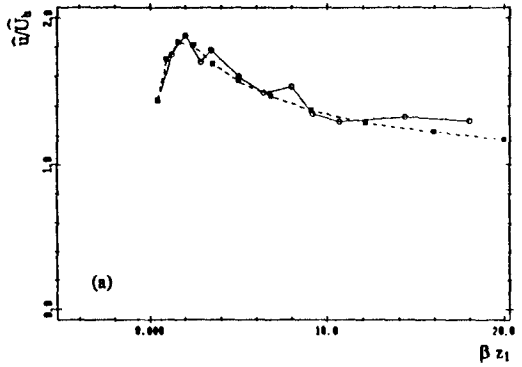

Fig. 11 Vertical variation of the amplitude of the velocity u calculated (- -) and measured (o——o) by Du Toit and Sleath (1981) above the crest.

At height z = 1.65 cm above the crest (Fig. 10), good agreement can be seen between the amplitude of the calculated and measured horizontal velocities u, as well as for the fluctuating horizontal velocity $\sqrt{u'^2}$. There is, however, a discrepancy of 25° between the measured local peak ($\omega t = 140°$) and that calculated ($\omega t = 165°$).

The vertical variation of the amplitude of the velocity u, designated by $\hat{u}$, obtained from the model coincides with that measured above the crest (Fig. 11). Note that the z axis is normalized by the parameter $\beta = \sqrt{\omega/2\nu} = 7.2$ cm^{-1} and z_1 is measured from the ripple crest.

III-3. *Comparison with the experimental results of Sato et al. (1987)*

The test parameters are the following:

- The ripple is asymmetric with $L_r = 12$ cm, $h_r = 2$ cm, $d = 0.02$ cm.
- The potential flow is a third-order Stokes wave ($T = 2\pi/\omega = 4$ s) :

$$U_h = -29{,}5\ (\cos \omega t + 0{,}258 \cos 2\omega t + 0{,}048 \cos 3\omega t)\ \text{(cm/s)}$$

For the modelling, after determining the amplitudes a_n and the phase shifts θ_n of the simulated ripple, we choosed a grid of 13x25 nodes with $\Delta X = 1$ cm, and ΔZ varying from 0.06 cm to 0.6 cm. The time step is $\Delta t = 0.011$ s. The upper limit is choosen at $Z_h = 6.5$ cm.

Figure 12 shows the comparison between the results of the model and those of the measurement for the velocity field and the turbulent kinetic energy K for phase $\omega t = 54°$. It can be seen that the vortex obtained with the model on the right hand leeside of the ripple is weaker than that measured, and the calculated intensity K is smaller in the model than found experimentally.

IV. DISCUSSION AND CONCLUSION

We have examined the problem of the oscillatory turbulent boundary layer on a rough sea bed using different versions of a turbulent closure model with two equations, one for the turbulent kinetic energy K and the other for the length scale L.

* *Performance of the model* : For a flat bed, a simplified three dimensional model was used to investigate the hydrodynamic characteristics of the flow in the boundary layer as a function of the different wave, current, angle of interaction and bed parameters. For the oblique wave-current interaction, the model requires further experimental verifications.

For a rippled bed, we have used a two-dimensional model that can reproduce the velocity and the vorticity fields as well as other turbulent quantities. Comparison with the experimental results shows that this model is able to predict quite well the complex flow properties over a rippled bed. Before applying the model to general cases, it would be necessary to confirm the numerical results by conducting further tests, particularly for the Reynolds stresses and the turbulent quantities.

* *Limitation of the model* : As for all models of turbulent closure (Rodi, 1980), the present model was originally designed for permanent flows in the fully developed turbulent regime at high Reynolds numbers. When the flow is oscillatory, the condition of local equilibrium of the turbulence, which is valid for a permanent flow,

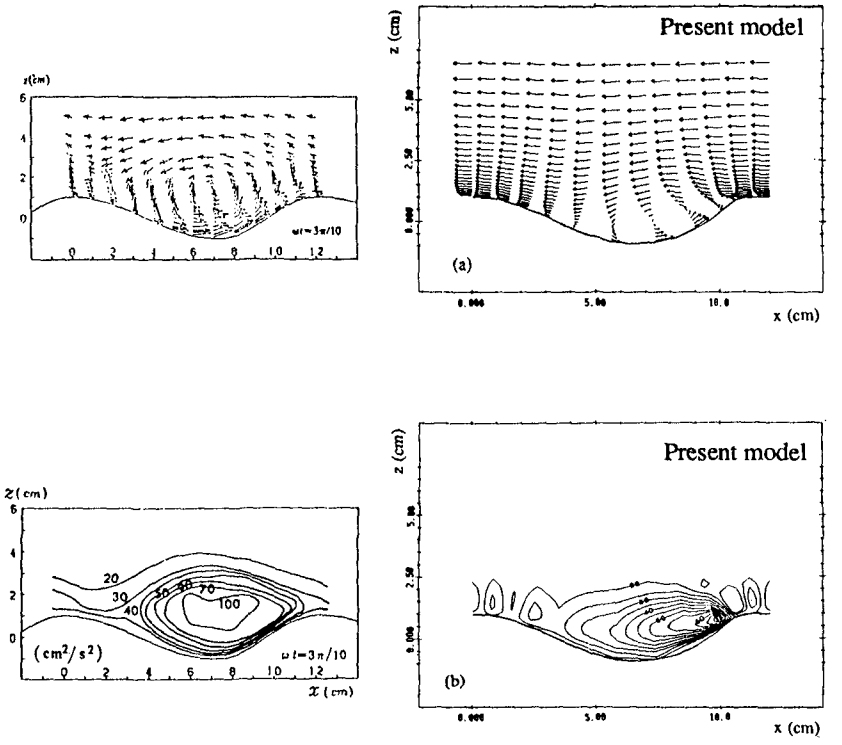

Fig. 12 Comparison between the results of the present model and the measurements of Sato et al. (1987) at phase $\omega t = 54°$.
(a) velocity field; (b) turbulent kinetic energy field

is no longer completely satisfied, particularly at the times when the velocity of the potential flow is small. Consequently there is a time variation of the friction in the oscillatory boundary layer, which induces the change of flow regime in the course of a period. No such change was included in the model. Thus, to obtain more precise results, it is necessary to improve the model not only for high Reynolds numbers but also for moderate Reynolds numbers.

In parallel with investigations into improvements, we shall apply the model to the prediction of certain important parameters of the natural boundary layer, together with analysis of sea measurements in the framework of the GDR Manche project.

REFERENCES

ASANO T. and IWAGAKI Y. (1984). *Proc. 16th Conf. Coastal Eng.*, pp. 2397 - 2413.

BAKKER W. T. (1974). *Proc. 14th Conf. Coastal Eng.*, pp. 1129 - 1148.

BAKKER W. T. and VAN DOORN Th. (1978). *Proc. 16th Conf. Coastal Eng.*, pp. 1394-1413.

BIJKER E. W. (1967). *Delft Hydraul. Lab.* Rep. 50.

BLONDEAUX P. (1987). *J. Hydraul. Res.*, 25 (4), pp. 447 - 463.

BREVIK I. (1981). *J. Waterway Port Coastal Ocean Div.*, 107 (WW 3), pp. 175 - 188.

DAVIES A. G., SOULSBY R. L. and KING H. L. (1988). *J. Geophys. Res.*, 93 (C1), pp. 491-508.

DU TOIT C. G. and SLEATH J. F. A. (1981). *J. Fluid Mech.*, 112, pp. 71 - 96.

FREDSOE J. (1984). *Inst. Hydrodyn. Hydraul. Eng. Tech. Univ. Denmark.* Series paper 35.

GRANT W. D. and MADSEN O. S. (1979). *J. Geophys. Res.*, 84 (C4), pp. 1797 - 1808.

HORIKAWA K. and WATANABE A. (1968). *Coastal Eng. Jpn.*, 11, pp. 13 - 28.

HUYNH THANH S. and TEMPERVILLE A. (1989). *Proc. 23th Cong. IAHR*, pp. A247-A254.

JENSEN B. L., SUMER B. M. and FREDSOE J. (1989). *J. Fluid Mech.*, 206, pp. 265 - 297.

JONSSON I. G. (1963). *Proc. 10th Congr. IAHR*, pp. 85 - 92.

JONSSON I. G. and CARLSEN N. A. (1976). *J. Hydraul. Res.*, 14 (1), pp. 45 - 60.

JONSSON I. G. (1980). *Ocean Eng.*, 7, pp. 109 - 152.

JUSTESEN P. (1988). *Coastal Eng.*, 12, pp. 257-284.

KAJIURA K. (1968). *Bull. Earthquake Res. Inst.*, 46, pp. 75 - 123.

KAMPHUIS J. W. (1975). *J. Waterw., Harbors Coastal Eng. Div.*, 101 (WW 2), pp. 135 - 144.

LEWELLEN W. S. (1977). In Handbook of turbulence, Plenum Publishing Corp., Vol. 1, pp. 237- 280.

MYRHAUG D. (1982). *Ocean Eng.*, 9, pp. 547 - 565.

PATANKAR S. (1980). Numerical heat transfer and fluid flows. McGraw Hill Book Co..

ROACHE P. J. (1976). Computational fluid dynamics. Eds. Hermosa Publishers.

RODI W. (1980). Turbulence models and their applications in hydraulics. Monograph, IAHR, Delft, The Netherlands.

SATO S., SHIMOSAKO K. and WATANABE A. (1987). *Coastal Eng. Jpn.*, 30, pp. 89 - 98.

SHENG Y. P. (1984). *Proc. 19th Conf. Coastal Eng.*, pp. 2380 - 2396.

SHENG Y. P. and VILLARET C. (1989). *J. Geophys. Res.*, 94 (C10), pp. 14,429 - 14,444.

SIMON R. R., KYRIACOU A., SOULSBY R. L. and DAVIES A. G. (1988). *IAHR Symposium on Mathematic Modeling of Sediment Transport in the Coastal Zone*, pp. 33 - 47.

SLEATH J. F. A. (1987). *J. Fluid Mech.*, 182, pp. 369 - 409.

SMITH J. D. (1977). In The Sea, vol. 6, Eds. Wiley-Interscience, New York, pp. 539 - 578.

SUMER B. M., JENSEN B. L. and FREDSOE J. (1986). In Advances in Turbulences, pp. 556-567.

TANAKA H. and SHUTO N. (1984). *J. Hydraul. Res.*, 22 (4), pp. 245 - 261.

VAN DOORN Th. (1981). *Delft Hydraul. Lab.* Rep. M1423. Part 1.